Electronic Supplementary Information

A trade-off between migration and association energies for hydride-ion conductivity in the $SrLiH_3$–$CaLiH_3$–$NaLiH_2$ system

Takashi Hirose,[a] Naoki Matsui,*[b] Kenta Watanabe,[a,b] Takashi Saito,[c,d] Kazuhiro Mori,[c] Kota Suzuki,[b] Masaaki Hirayama*[a,b] and Ryoji Kanno*[b]

[a]Department of Chemical Science and Engineering, School of Materials and Chemical Technology, Institute of Science Tokyo, 4259 Nagatsuta, Midori–ku, Yokohama 226–8501, Japan

[b]Research Center for All–Solid–State Battery, Institute of Integrated Research, Institute of Science Tokyo, 4259 Nagatsuta, Midori–ku, Yokohama 226–8501, Japan

[c]Neutron Science Division (KENS), Institute of Materials Structure Science, High Energy Accelerator Research Organization (KEK), 203–1 Shirakata, Tokai, Ibaraki 319–1106, Japan

[d]Department of Materials Structure Science, School of High Energy Accelerator Science, The Graduate University for Advanced Studies, SOKENDAI, 203–1 Shirakata, Tokai, Ibaraki 319–1106, Japan

*Corresponding author.

Email: Naoki Matsui, matsui.n.ee49@m.isct.ac.jp

Masaaki Hirayama, hirayama@mac.titech.ac.jp

Ryoji Kanno, kanno.r.ade9@m.isct.ac.jp

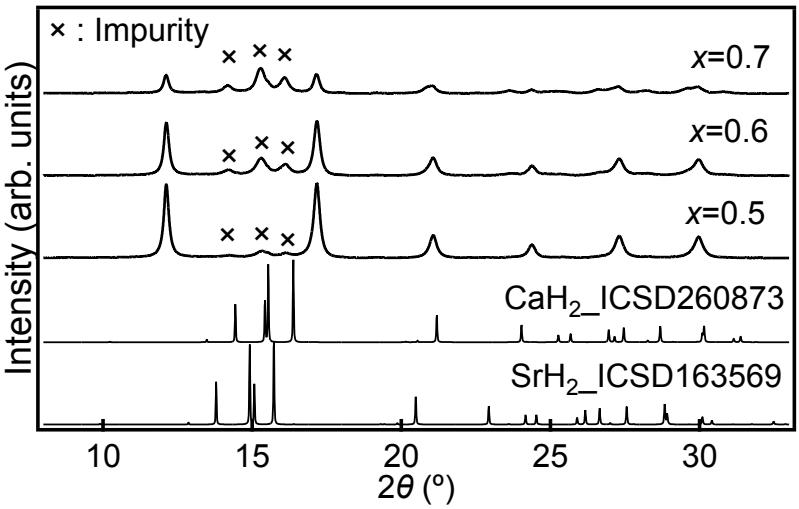

Figure S1. Impurities of $Sr_{1-x}Ca_xLiH_3$ ($0.5 \leq x \leq 0.7$).

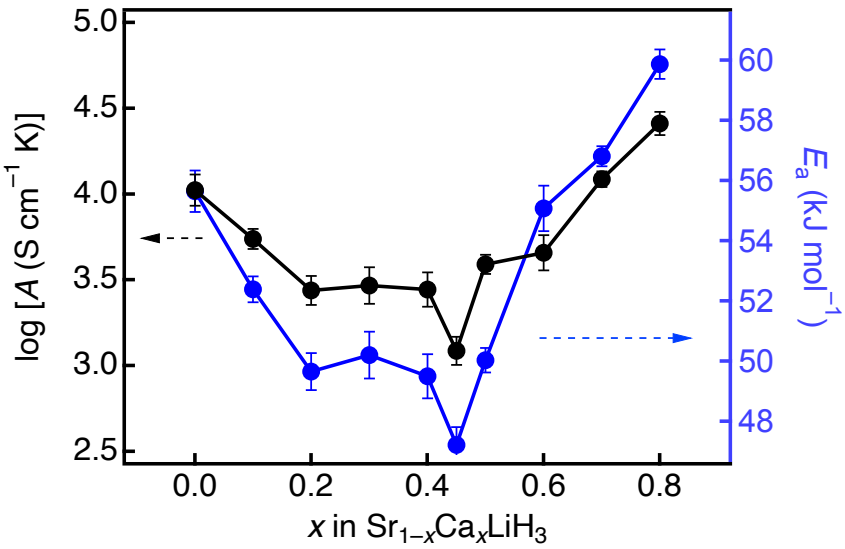

Figure S2. The pre-exponential factor and activation energy versus Ca amount in $Sr_{1-x}Ca_xLiH_3$.

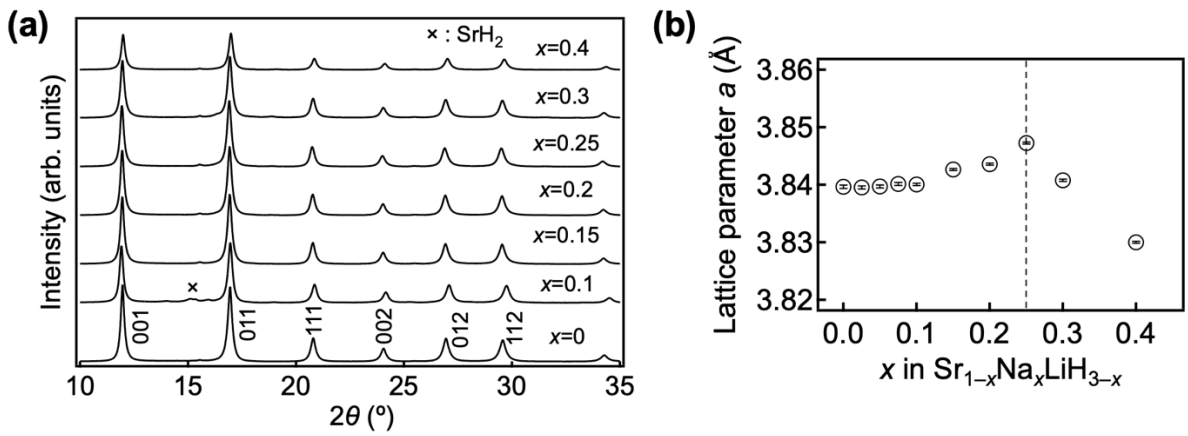

Figure S3. (a) Synchrotron XRD patterns and (b) lattice parameters of $Sr_{1-x}Na_xLiH_{3-x}$ ($0 \leq x \leq 0.4$) samples ball milled for 12 hours.

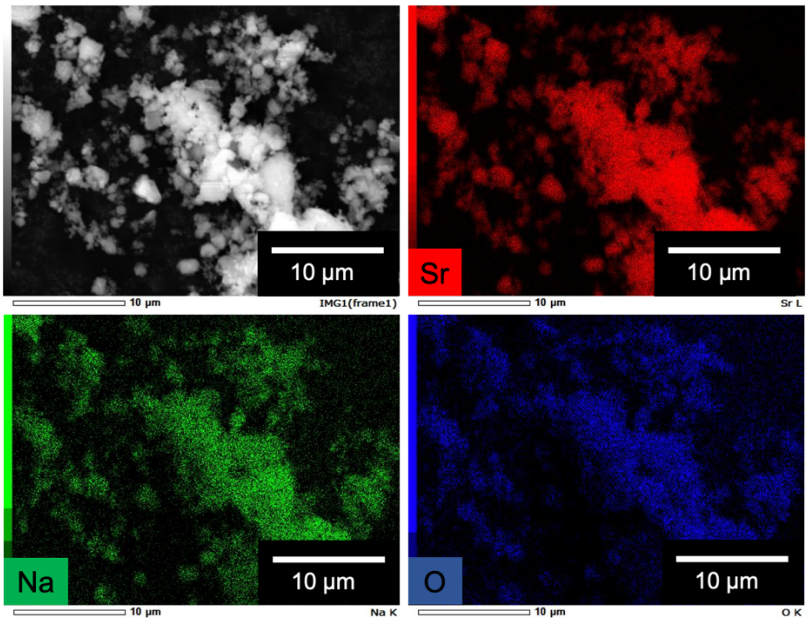

Figure S4. SEM image and EDX mapping of $Sr_{0.8}Na_{0.2}LiH_{2.8}$.

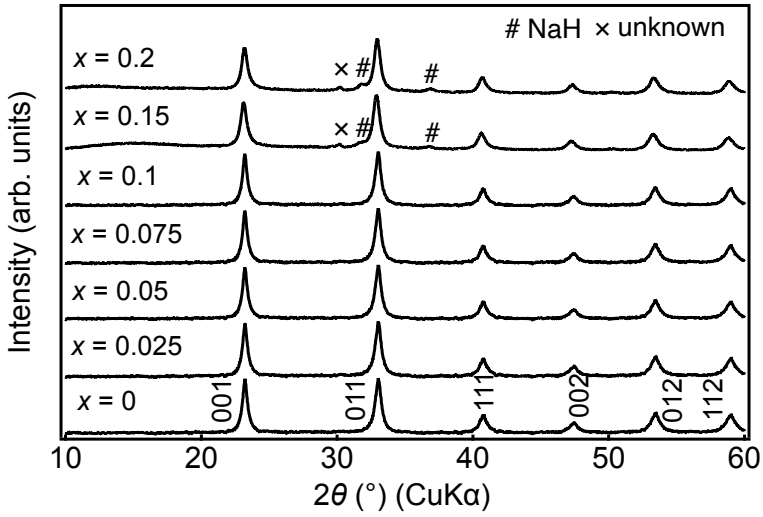

Figure S5. XRD patterns of $Sr_{1-x}Na_xLiH_{3-x}$ samples ball milled for 3 hours. The results for $0 \leq x \leq 0.1$ were cited from the previous study.[1]

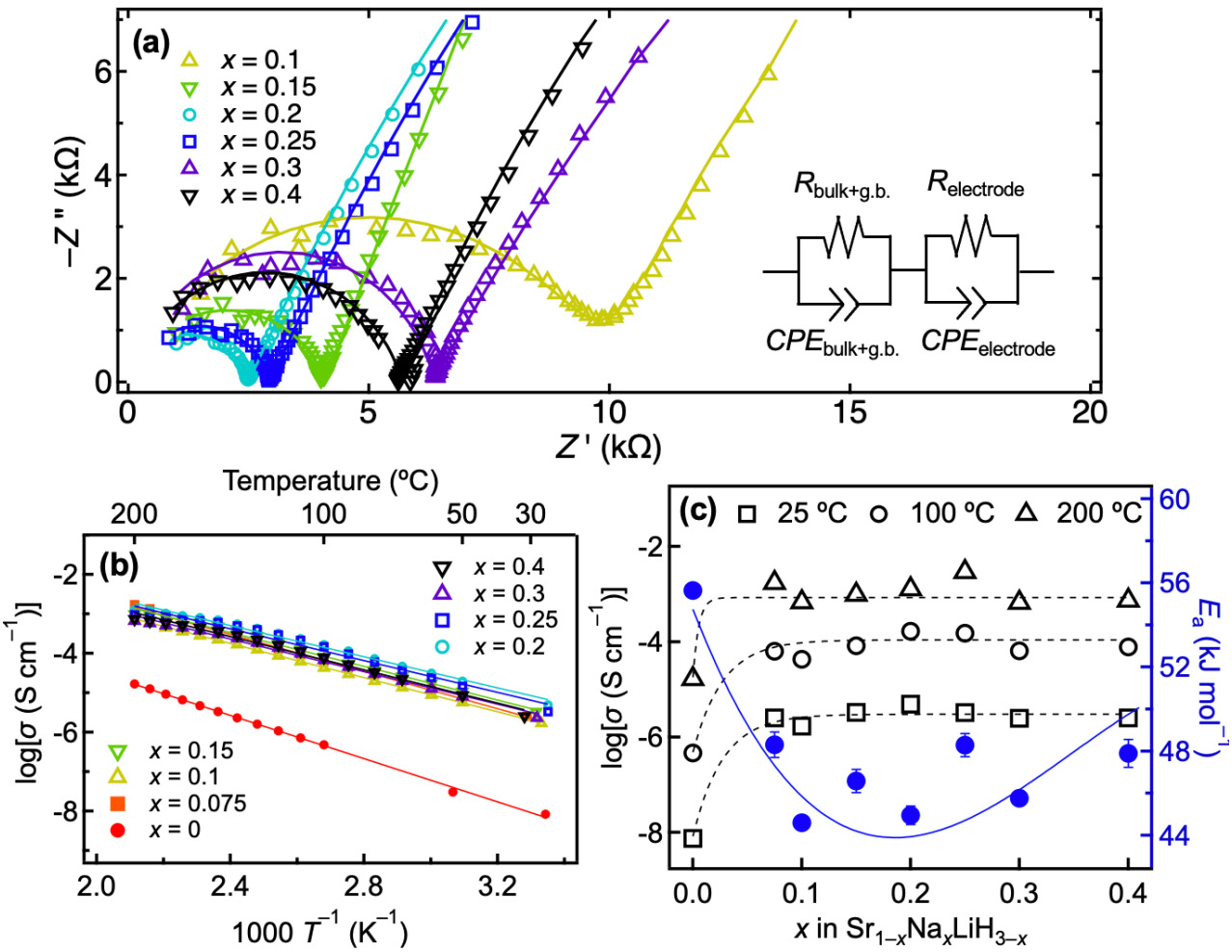

Figure S6. (a) Nyquist plots of $Sr_{1-x}Na_xLiH_{3-x}$ ($0.1 \leq x \leq 0.4$) at 100 °C. The inset shows the equivalent circuit used for fitting. (b) Arrhenius plots of the total ionic conductivity for $Sr_{1-x}Na_xLiH_{3-x}$ ($0.1 \leq x \leq 0.4$) samples. (c) Ionic conductivity and activation energy versus nominal Na amount in $Sr_{1-x}Na_xLiH_{3-x}$. The activation energy is shown as blue circles against the right axis.

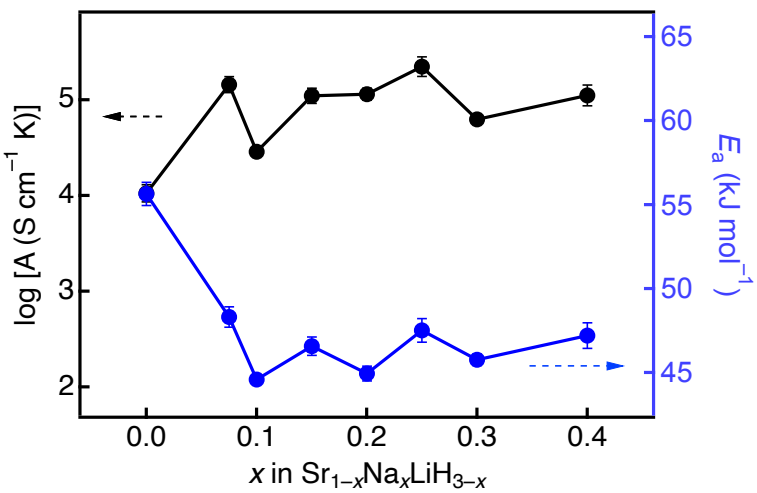

Figure S7. The pre-exponential factor and activation energy versus Na amount in $Sr_{1-x}Na_xLiH_{3-x}$.

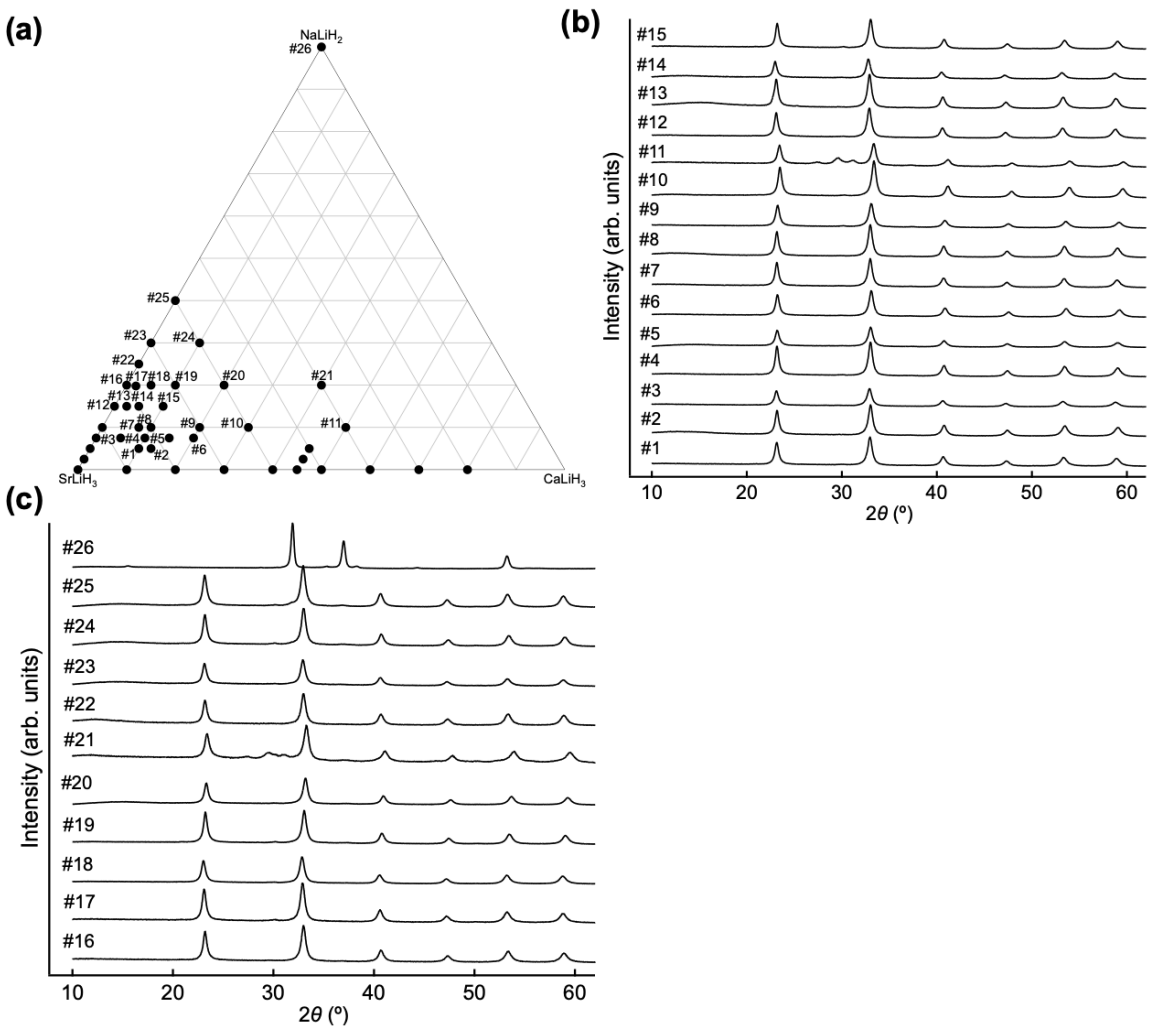

Figure S8. (a) Synthesised compositions are indicated by the black points in the $SrLiH_3$–$CaLiH_3$–$NaLiH_2$ pseudo-ternary diagram. The XRD patterns of the samples (b) No. 1–15 and (c) No. 16–26.

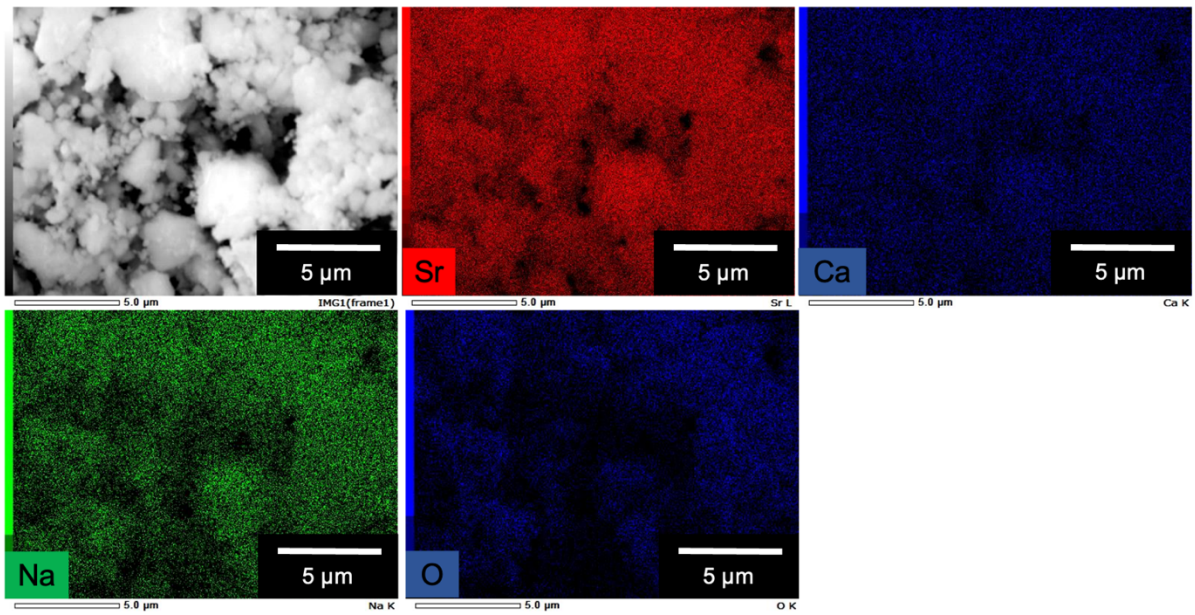

Figure S9. SEM image and EDX mapping of $Sr_{0.7}Ca_{0.1}Na_{0.2}LiH_{2.8}$.

Table S1. Several perovskite-type hydride-ion conductors showing high performance in the $SrLiH_3$–$CaLiH_3$–$NaLiH_2$ pseudo-ternary system and their ionic conductivities and activation energies.

composition	$\sigma_{r.t.}$ [S cm^{-1}]	$\sigma_{100\,°C}$ [S cm^{-1}]	E_a [kJ mol^{-1}]
$Sr_{0.8}Na_{0.2}LiH_{2.8}$	5.1×10^{-6}	1.7×10^{-4}	45.0
$Sr_{0.7}Ca_{0.1}Na_{0.2}LiH_{2.8}$	4.2×10^{-6}	4.6×10^{-5}	45.1
$Sr_{0.75}Ca_{0.1}Na_{0.15}LiH_{2.85}$	3.7×10^{-6}	1.2×10^{-4}	47.0
$Sr_{0.78}Ca_{0.02}Na_{0.2}LiH_{2.8}$	3.7×10^{-6}	1.1×10^{-4}	43.8
$Sr_{0.825}Ca_{0.075}Na_{0.1}LiH_{2.9}$	3.5×10^{-6}	1.1×10^{-4}	45.5
$Sr_{0.925}Na_{0.075}LiH_{2.925}$	1.9×10^{-6}	6.4×10^{-5}	46.3
$Sr_{0.825}Ca_{0.025}Na_{0.15}LiH_{2.85}$	7.0×10^{-7}	1.7×10^{-5}	41.8
$Sr_{0.725}Ca_{0.2}Na_{0.075}LiH_{2.925}$	3.4×10^{-7}	3.2×10^{-5}	43.8

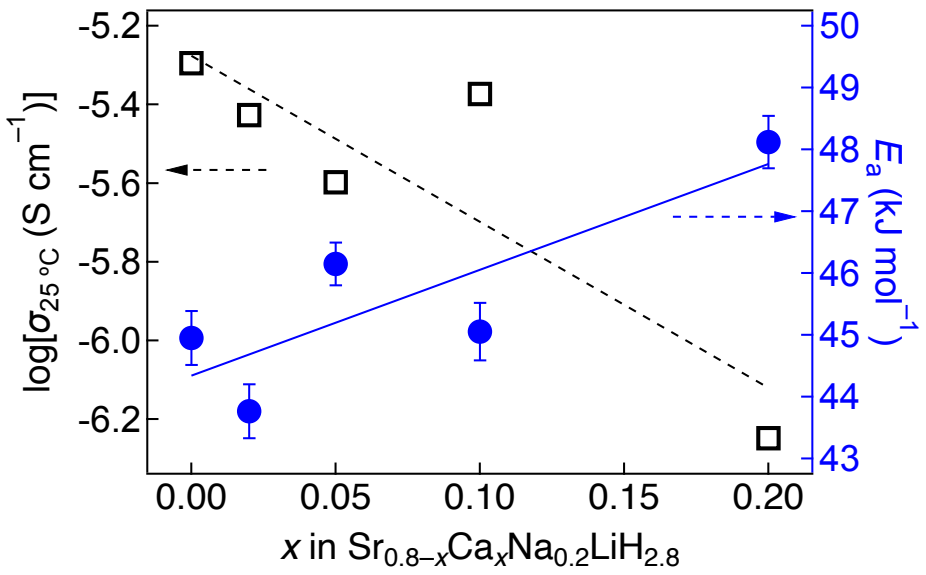

Figure S10. Plot of ionic conductivity at 25 °C and activation energy versus Ca dopant amount in $Sr_{0.8-x}Ca_xNa_{0.2}LiH_{2.8}$.

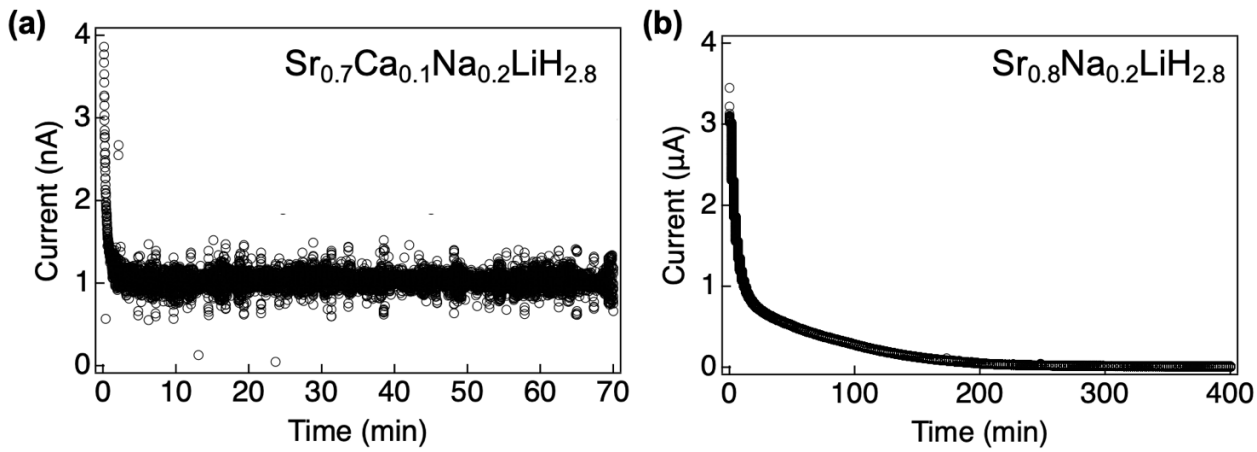

Figure S11. Time variation of the current change at an applied voltage of 50 mV using a Mo|SE|Mo symmetric cell obtained by direct current (DC) measurement at 50 °C; (a) $Sr_{0.7}Ca_{0.1}Na_{0.2}LiH_{2.8}$ and (b) $Sr_{0.8}Na_{0.2}LiH_{2.8}$.

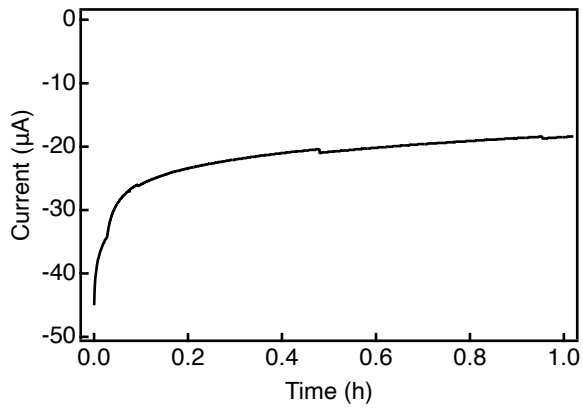

Figure S12. Current *vs.* Time curve from DC polarization measurements using a (–)Mo|Ti+TiH_2+$Sr_{0.8}Na_{0.2}LiH_{2.8}$+AB|$Sr_{0.8}Na_{0.2}LiH_{2.8}$|$TiH_2$+$Sr_{0.8}Na_{0.2}LiH_{2.8}$+AB|Mo(+) cell at 50 ºC. The relaxation time was 1 hour. The applied voltage was –0.3 V *vs.* OCV. The Ti composite electrode or Ti/TiH_2 composite electrode was synthesized under the conditions of 100 rpm for 8 hours with weight ratios of TiH_2:SE:AB = 20:75:5 wt.% and Ti:TiH_2:SE:AB = 12:8:75:5 wt.%, respectively.

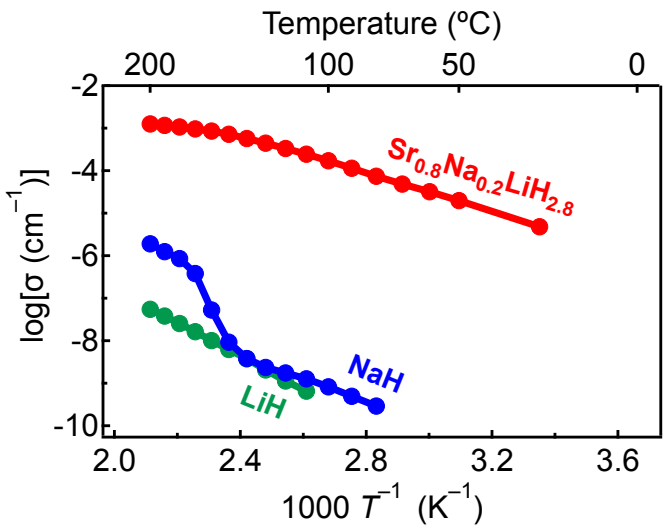

Figure S13. Arrhenius plots of $Sr_{0.8}Na_{0.2}LiH_{2.8}$, LiH, and NaH.

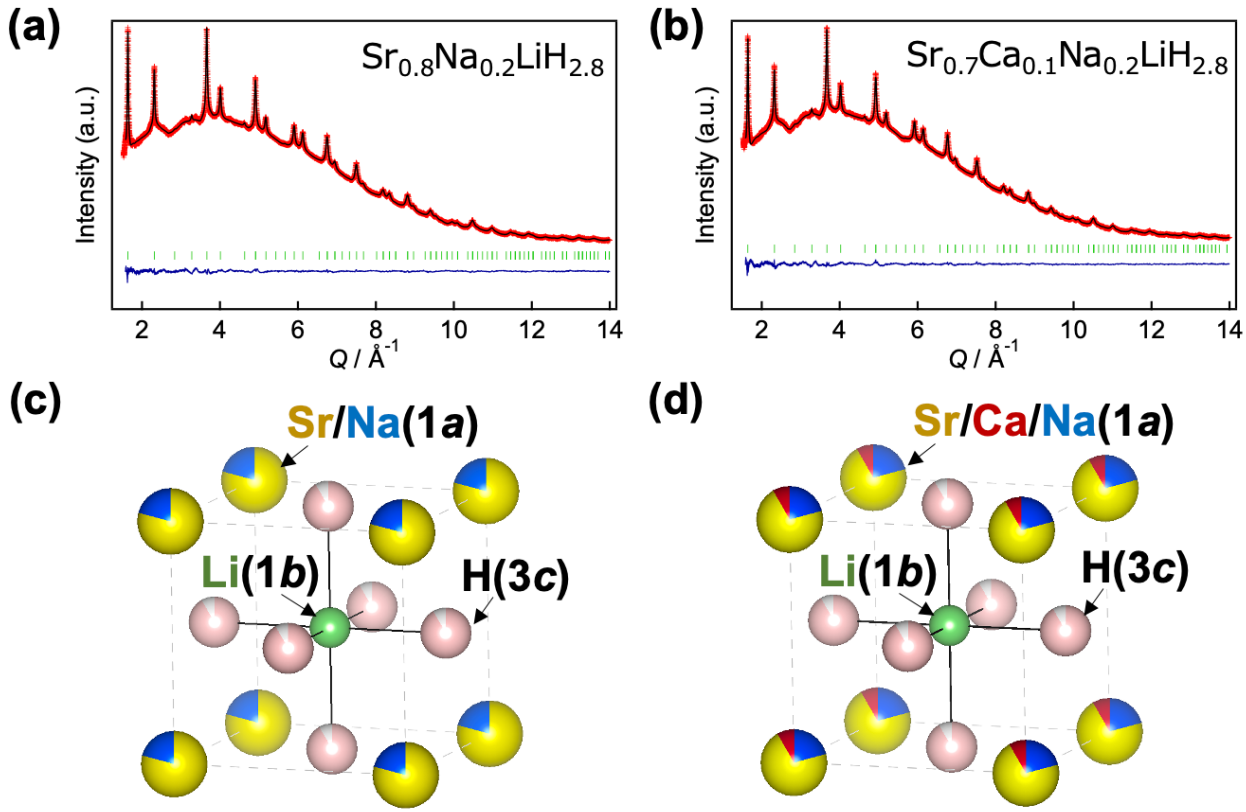

Figure S14. Neutron Rietveld refinement profiles of (a) $Sr_{0.8}Na_{0.2}LiH_{2.8}$ and (b) $Sr_{0.7}Ca_{0.1}Na_{0.2}LiH_{2.8}$. The refined structure of (c) $Sr_{0.8}Na_{0.2}LiH_{2.8}$ and (d) $Sr_{0.7}Ca_{0.1}Na_{0.2}LiH_{2.8}$.

Table S2. Rietveld refinement results of Neutron diffraction patterns of (a) $Sr_{0.8}Na_{0.2}LiH_{2.8}$ and (b) $Sr_{0.7}Ca_{0.1}Na_{0.2}LiH_{2.8}$.

(a)$Sr_{0.8}Na_{0.2}LiH_{2.8}$

Atom	Site	g	x	y	z	B_{eq} / Å^2	B_{11} / Å^2	B_{22} / Å^2	B_{33} / Å^2
Sr	1*a*	0.819(11)	0	0	0	0.38(2)	0.38(2)	$=U_{11}$(Sr)	$=U_{11}$(Sr)
Na	1*a*	=1–g(Sr)	0	0	0	0.38(2)	$=U_{11}$(Sr)	$=U_{11}$(Sr)	$=U_{11}$(Sr)
Li	1*b*	1	0.5	0.5	0.5	0.84(3)	0.84(3)	$=U_{11}$(Li)	$=U_{11}$(Li)
H	3*c*	0.930(8)	0.5	0.5	0	2.30(4)	2.46(7)	$=U_{11}$(H)	1.98(5)

Unit cell: Cubic *Pm*–3*m* (221); $a = b = c = 3.83868(3)$ Å, $V = 56.5296(13)$ Å^3; R_{wp} =0.426%, R_e = 0.19%, R_p = 0.32%, R_B =1.87%, R_F = 2.22%, goodness of fit $S = R_{wp}/R_e = 2.19$.

(b)$Sr_{0.7}Ca_{0.1}Na_{0.2}LiH_{2.8}$

Atom	Site	g	x	y	z	B_{eq} / Å^2	B_{11} / Å^2	B_{22} / Å^2	B_{33} / Å^2
Sr	1*a*	0.703(5)	0	0	0	0.47(3)	0.47(3)	$=U_{11}$(Sr)	$=U_{11}$(Sr)
Ca	1*a*	0.106(18)	0	0	0	0.47(3)	$=U_{11}$(Sr)	$=U_{11}$(Sr)	$=U_{11}$(Sr)
Na	1*a*	0.192(24)	0	0	0	0.47(3)	$=U_{11}$(Sr)	$=U_{11}$(Sr)	$=U_{11}$(Sr)
Li	1*b*	1	0.5	0.5	0.5	0.85(3)	0.85(3)	$=U_{11}$(Li)	$=U_{11}$(Li)
H	3*c*	0.936(14)	0.5	0.5	0	2.34(4)	2.88(8)	$=U_{11}$(H)	1.25(6)

Unit cell: Cubic *Pm*–3*m* (221); $a = b = c = 3.82772(3)$ Å, $V = 56.0404(13)$ Å^3; R_{wp} =0.378%, R_e = 0.20%, R_p = 0.28%, R_B =1.93%, R_F = 3.67%, goodness of fit $S = R_{wp}/R_e = 1.88$.

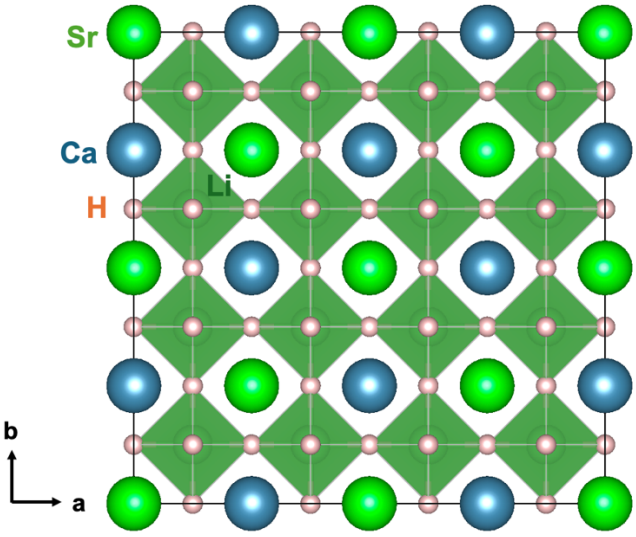

Figure S15. The crystal structure of $Sr_{0.5}Ca_{0.5}LiH_3$ used in the theoretical calculations.

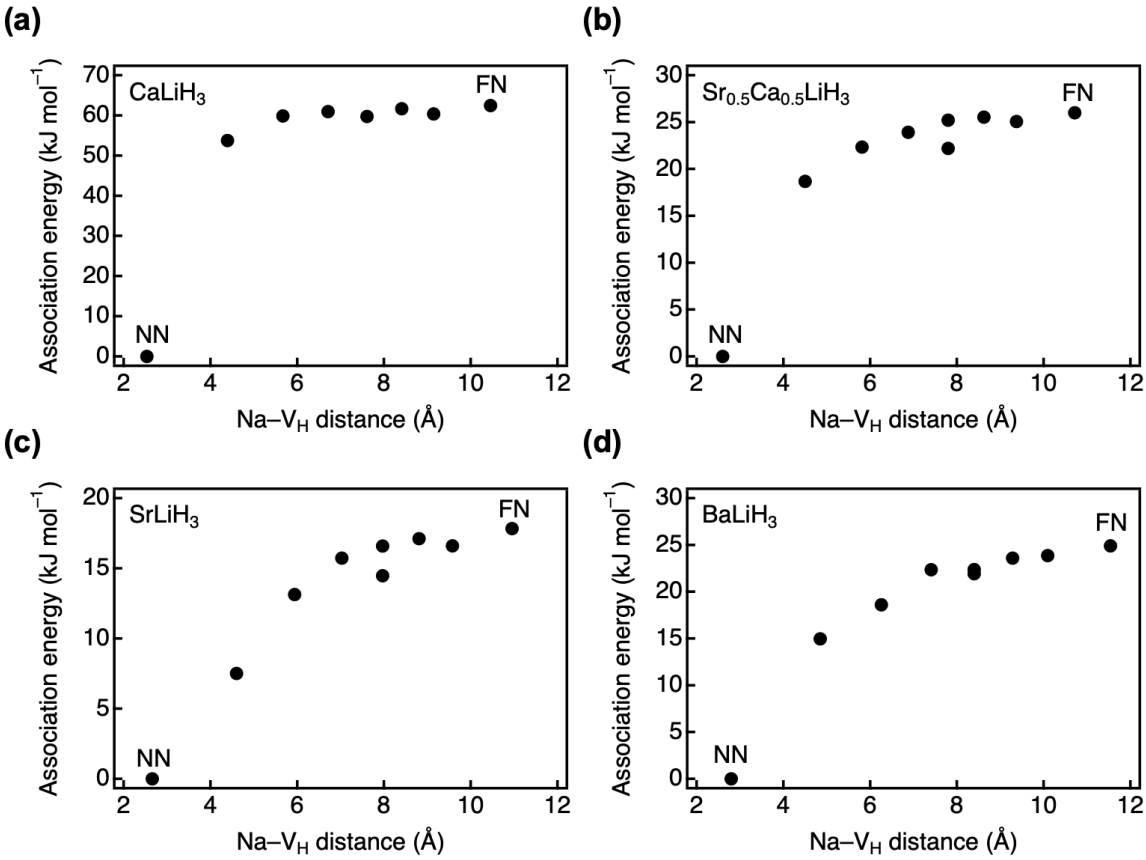

Figure S16. The association energy of (a)$CaLiH_3$, (b)$Sr_{0.5}Ca_{0.5}LiH_3$, (c)$SrLiH_3$, and (d)$BaLiH_3$.

References

1. T. Hirose, T. Mishina, N. Matsui, K. Suzuki, T. Saito, T. Kamiyama, M. Hirayama and R. Kanno, *ACS Appl. Energy Mater.*, 2022, **5**, 2968-2974.